



Integrated three-dimensional visualization and soft-sensing system for underground paste backfilling



Zhaolin Yuan^b, Xiaojuan Ban^{a,b,e,*}, Fangyuan Han^b, Xingquan Zhang^d, Shenghua Yin^c, Yiming Wang^c

^a Beijing Advanced Innovation Center for Materials Genome Engineering, Institute of Artificial Intelligence, University of Science and Technology Beijing, Beijing 100083, China

^b School of Computer and Communication Engineering, University of Science and Technology Beijing, Beijing 100083, China

^c School of Civil and Resource Engineering, University of Science and Technology Beijing, Beijing 100083, China

^d Institute of Automation, Chinese Academy of Sciences

^e Beijing Key Laboratory of Knowledge Engineering for Materials Science, Beijing 100083, China

ARTICLE INFO

Keywords:

goaf
Soft-sensing
3D visualization system
Laser scanning
Volume calculation

ABSTRACT

Cemented paste backfilling (CPB) has attracted worldwide attention because of its advantages in the processing of waste tailings and underground goafs. A problem of the underground CPB procedure that has received little attention is the shortage of devices or techniques for monitoring the real-time backfilling process accurately due to the harsh underground environment. Imprecise information of the backfilling progress will mislead the operators to make improper decisions, such as not pausing the transport system promptly or tuning the ratio of cement to tailings incorrectly. This study proposes a 3D visualization and soft-sensing system for the cemented paste backfilling process. By employing a GeoSLAM ZEB-HORIZON laser scanner to scan the 3D model of the underground goaf, the system estimates the backfilling height in real-time according to the accumulated volume of filled paste and simulates the backfilling of the underground goaf on web pages. In a real Copper Mine, we examined the developed system and soft-sensing technique in goafs and found that the relative error of estimated backfilling height is under 10%, which is acceptable in real production. The results indicate that the developed backfilling visualization and the soft-sensing techniques provide significant guidance for production management in underground backfilling.

1. Introduction

In modern mining, the paste backfilling technique (Lu et al., 2018) is an advanced waste tailing processing method for recycling the by-products of mineral excavation. This technology maximizes the utilization of industrial solid waste (tailings, waste rock, slag, and phosphogypsum) and controls the movement of the surrounding rock. The detailed process of the paste backfilling procedure is illustrated in Fig. 1. Cemented paste is produced by bonding tailings, cement, or other hydraulic binders and water at the maximum concentration. These mixtures are transported into underground goafs through pumping or gravity (Yin et al., 2020).

Most researchers have studied the three main processes of paste technology: thickening (Yuan et al., 2020; Núñez et al., 2020; Wu et al.,

2020), mixing preparation (Qi et al., 2018; Li et al., 2019), and transportation (Qi et al., 2018), which significantly affect the paste quality and financial cost. This paper presents and solves a problem of the cemented paste backfilling procedure that attracts little attention and has not been addressed previously. In most underground mines, it lacks adequate techniques to monitor the real time progress of backfilling tasks for goaf, including the paste height, composition, and remaining time for backfilling. Although some previous studies (Wang et al., 2019; Mishra et al., 2018) introduce wireless remote measurement and multi-sensor to monitor the state of discarded underground goafs, such solutions are not appropriate for backfilling monitoring. The primary difficulty is that the internal space of a goaf will be filled with the cemented paste after backfilling, and thus, any devices and sensors installed in the goaf can never be recycled. In addition, installing sensors and additional

* Corresponding author.

E-mail addresses: b20170324@xs.ustb.edu.cn (Z. Yuan), banxj@ustb.edu.cn (X. Ban), hfy@xs.ustb.edu.cn (F. Han), zhangxingquan2022@ia.ac.cn (X. Zhang), csuys@126.com (S. Yin), ustbwym@126.com (Y. Wang).

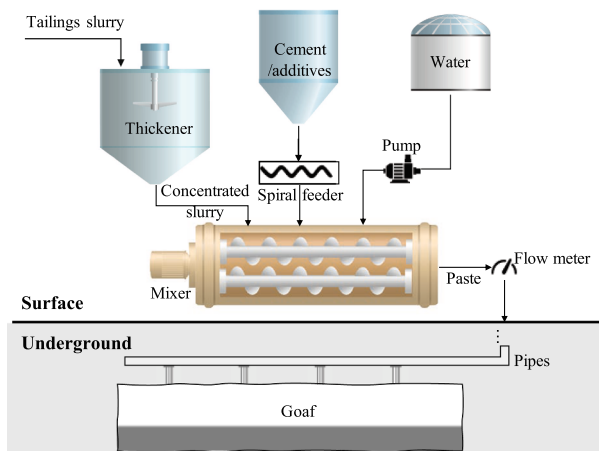


Fig. 1. Typical diagram of paste backfilling.

support equipment for communication is extremely difficult and expensive in an underground environment. Generally, engineers only measured the height and progress of backfilling manually and discontinuously when the back-filling system is paused and the filled paste has been solidified. The inaccurate and non-real-time estimation of the backfilling progress has two adverse effects in backfilling management:

- The operators in the paste production station cannot judge whether it is time to shut the paste pumping system down. For example, the backfilling mission is completed and the operator should stop backfilling to achieve accurate roof contact (Lu and Zhang, 2017) and reduce the waste of cemented paste. The second example is pausing the backfilling and waiting for the paste to be solidified for preserving the retaining wall when the paste height reaches the setpoint.
- Generally, with the increase in the backfilling height, the required strength of the cemented paste may decline slightly. A lower dosage of cement reduces the backfilling cost significantly. As a vital indicator that guides the operators in paste production stations to adjust the cement-tailings ratio, the backfilling height is not measured accurately in most paste backfilling stations.

Generally, some other industrial productions also face the problems of difficult monitoring, which are usually confronted by some informational techniques, such as simulation, visualization, and soft-sensoring. Chen et al. (2014) developed a 3D monitoring alarm warning system for tunnel construction. The system provided the 3D interactive operation, monitoring data analysis, and automatic alarm warning, which improved the safety status analysis of visual construction site monitoring. A mine water-inrush visualization simulation system (Zhou et al., 2012) was designed for the underground mining environment to simulate the water-inrush disaster process, which provided guidance for the operators to take action to improve mining safety. Based on the GIS technology and 3D visualization technology, Hu et al. (2013) implemented a digital ventilation system for an actual mine. As critical components of the digital twin system (Tao et al., 2018; Fuller et al., 2020; Liu et al., 2021), real-time visualization and soft-sensoring are future-oriented techniques for achieving the goal of Industry 4.0 (Vachalek et al., 2017) in modern production.

In this paper, from the perspectives of actual backfilling requirements and the development tendency in industrial techniques, we propose a novel pipeline to achieve the soft-sensing of the backfilling progress and visualize the real-time backfilling in a three-dimensional platform. We first utilize a sophisticated laser radar instrument to collect the complete point cloud data of the goaf (LUO et al., 2016). After preprocessing the dense point cloud, we slice the goaf evenly along the

height-axis and compute the volume for each slice. When the paste backfilling begins, we accumulate the volume of the fed paste and find the corresponding slice to estimate the backfilling height in real time. In addition, the most appropriate cement–sand ratio is also recommended based on the current backfilling height and the technical parameters. Furthermore, an integrated three-dimensional visualization system is developed based on the Browser/Server (B/S) architecture, which visualizes the filled goaf and progress information from three dimensional perspective in real time for the operators.

2. Method

To achieve the graphical simulation and soft-sensoring of the backfilling procedure, a systematic pipeline is illustrated in Fig. 2. It includes the hardware, data collecting, data preprocessing, backfilling simulation, and the development of the human-computer interface. First, we adopted a laser scanner to collect the complete 3D point cloud model of the goaf. Next, we cut the original goaf model into slices, cut each slice into blocks successively, and estimate the volume for each block based on Monte Carlo sampling. We sum up the volumes of blocks belonging to the same slice and estimate the volume for each slice. Finally, an associative table of the correlation between backfilling height and volume was generated according to the volume and height of each slice. Based on the generated associative table, we estimate the backfilling height by taking advantage of the known accumulative volume of filled paste in real time. An integrated system based on the B/S framework is developed to produce vivid animations of the backfilling progress and represent key information simultaneously.

2.1. Three-dimensional point cloud scanning for goafs

To collect accurate 3D models of the filled goafs, traditional devices for underground surveying and mapping, such as the total station (Cosser et al., 2003), cannot meet the requirements for sophisticated measurement and visualization. In this project, we employed an advanced 3D laser scanner, ZEB-Horizon, which was produced by the Geo-Slam company for geological mapping. This instrument was composed of a laser lidar, electric machinery, and a handle. The effective scanning range was 100 m, which was suitable for the underground scanning of tunnels and goafs. When the device was operating, the laser continuously rotated to scan the three-dimensional point cloud of the underground environment completely.

We utilized the software **Geo-Slam Hub** to analyze the original 3D data and build the aligned point cloud with scanning trajectories. This step is called point cloud registration. After generating the 3D model using Geo-Slam Hub, the first task was to align the relative positions of the points to the absolute coordinate system. Before we started to scan the goaf, we set at least three measurement control points whose deterministic absolute coordinates were measured manually. These measurement control points with absolute coordinates identified a unique affine transformation, including a translation vector and a rotation matrix, to transform the scanned points cloud into absolute coordinate space.

Normally, the original point cloud model built from Geo-Slam Hub is extremely dense, which brings a computational burden for subsequent calculations. Empirically, we diluted the dense point cloud to a sparse one and constrained the distance between adjacent points to be approximately equal to 1 dm. Furthermore, we eliminated the internal noisy points in the goaf manually, including the effects from people, vehicles, and entities other than the real rock bodies. The operations including coordinate registration and down-sampling were conducted in the **CloudCompare** software. We eliminated noisy points using the **Geomatic** software.

We introduced the scanning process of the 3D point cloud model of the goaf with the laser scanner and preprocessing of the 3D point cloud model. The point cloud registration aligned the relative positions of the

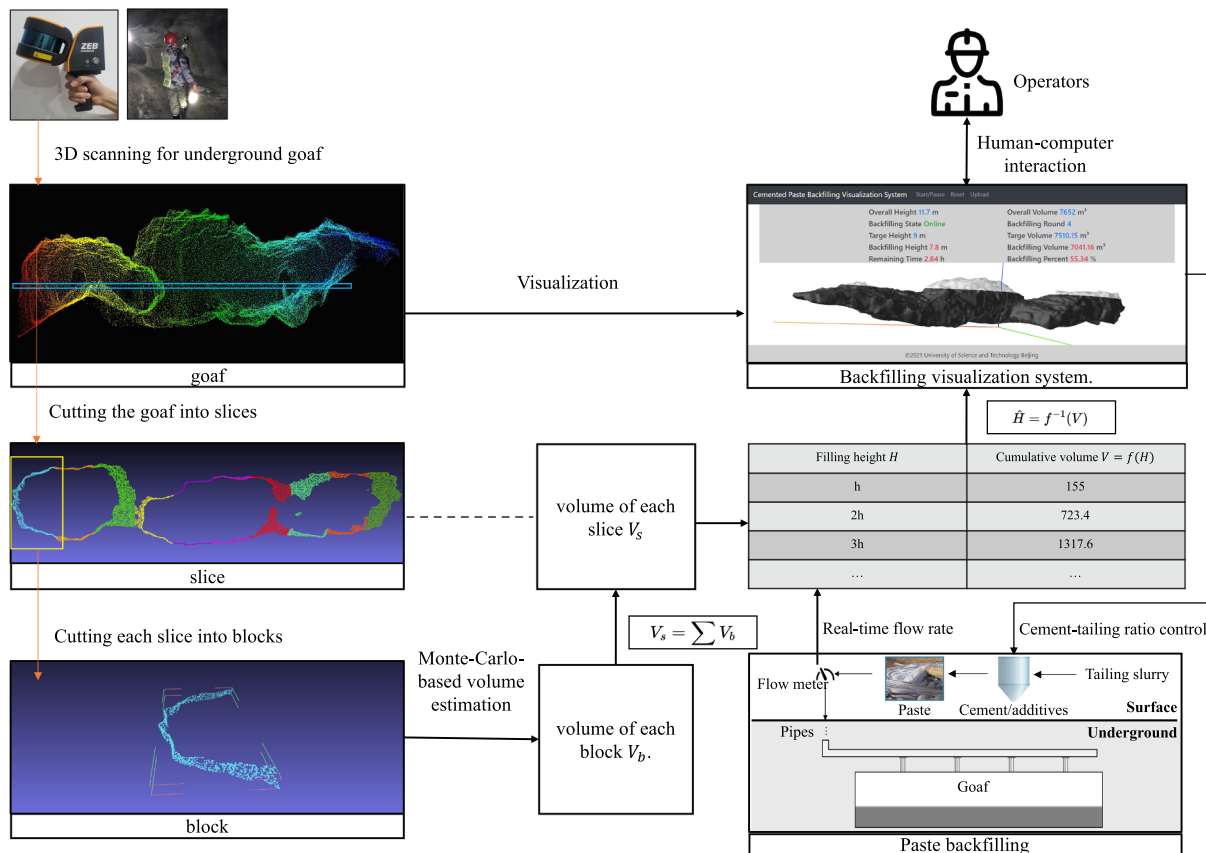


Fig. 2. Pipeline of this research.

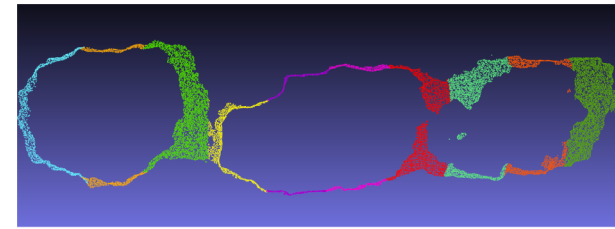
collected points to the absolute coordinate system, which effectively calibrated the direction of gravity and allowed us to cut the goaf model along the correct direction of gravity for accurate filling height estimation. However, it is unnecessary to hold the absolute coordinates in the visualization system when we only focus on a single goaf instead of the relationship between the target goaf and surrounding environment. Therefore, we transformed the model from the absolute coordinate system to the appropriate relative coordinate system with guaranteeing the direction of gravity was constant.

In the actual production, we find that the length of the studied goaf was significantly larger than its width and height. Therefore, we rotated the model along Z-axis to force the length side to be approximately parallel to the X-axis for the best visual experience after moving the model to the origin of the coordinates.

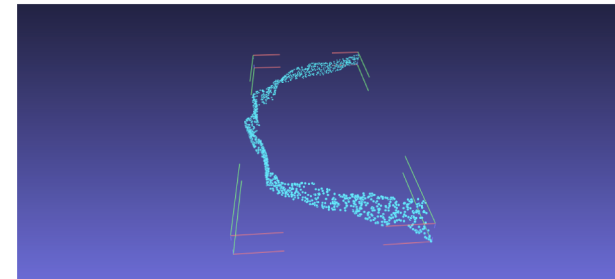
2.2. Slicing and volume calculation for goaf model

When the backfilling system was operating, the accumulated volume of filled paste in the goaf was estimated. An associative table that recorded the correlation between the paste volume and height in a specific goaf was constructed, which is utilized to estimate the backfilling height according to accumulated volume of discharged paste in real time.

Intuitively, we could construct the associative table by cutting the goaf into small slices evenly along the height direction and calculating the volume of each slice. However, the shape of the goaf was non-convex. As a result, there were some vacancies in the slices, which increased the difficulties in calculating the slice volume. As shown in Fig. 3(a), the slice with vacancies was concentrated at the bottom and top regions of the goaf. It was extremely difficult to estimate the volume of a slice accurately that was discontinuous and filled with holes. A multiple-cutting process was proposed to improve the accuracy of the



(a) Cutting the complete goaf into slices along the Z-axis.



(b) Cutting one slice into blocks along the X-axis.

Fig. 3. Multiple-cutting process for goaf model along Z-axis and X-axis.

estimated volume for such slices with vacancies. After cutting the goaf along the Z-axis, we attempted to cut each slice into small blocks along the X-axis successively. We built several planes that were perpendicular to the X-axis, the direction of the side length in the goaf, to cut each slice into blocks set. Fig. 3(b) illustrates the left-most block of the original slice in Fig. 3(a). Compared with a slice with many vacancies, the points in the block were continuous. We estimated the volume of each slice

indirectly by tallying up the volumes of all the blocks.

Next, we introduce the procedure for estimating the volume of each small non-closed block. Generally, based on the format of 3D models, the methods for calculating the volume for an irregular geometry are divided into mesh models and point cloud models. The methods based on mesh models assume the mesh model is enclosed, which requires reconstructing the point cloud to mesh model and patching the non-closed surface. However, as shown in Fig. 3(b), the surface at the top, bottom, and some side faces were all missing because of the multiple-cutting operation, which made reconstructing the surface of the block extremely difficult. Therefore, a point-cloud-based algorithm was adopted to estimate the volume of each block directly to avoid the requirement of three-dimensional reconstruction.

The method was implemented based on Monte Carlo sampling using the following steps:

1. An axis-aligned cuboid bounding box was constructed, as shown in Fig. 3(b), for points in the block, and the volume V of the box was calculated.
2. The points in the bounding box were sampled randomly N times, and the number of times X that the samples were located inside the point cloud block was counted.
3. The volume of the block, $\hat{V}_g = \frac{V \cdot X}{N}$, and the deviation of the estimation, $\sqrt{\frac{VV_g - V^2}{N}}$, were estimated based on statistics.

The key issue is to judge whether one sampled point is inside or outside of the non-closed point cloud block. We introduced the inside–outside classification method from Adams and Dutré (2003) to solve this classification problem.

Fig. 4 shows a simple example of the inside–outside classification. p_1 is a vertex of the triangular pyramid, s_2 is inside the pyramid, and s_1 is outside the model. Among all the vertices in the triangular pyramid, p_1 is the nearest point to s_1 and s_2 . We define the normal vector of the pyramid at p_1 as \vec{n} , which is the average of the normal vectors of the adjacent faces around p_1 , including \vec{n}_1 , \vec{n}_2 , and \vec{n}_3 . Whether the given point s_1 is inside or outside the model can be judged by calculating the inner product between $\vec{p_1 s_1}$ and \vec{n} . For instance, the inner product $\vec{p_1 s_1} \cdot \vec{n} \geq 0$ corresponds to an angle between the two vectors of 0° – 90° , which means that the point s_1 is outside of the model. For the point s_2 , because p_1 is an acute or obtuse angle vertex in the triangular pyramid, the inner product $\vec{p_1 s_2} \cdot \vec{n} \leq 0$ is not sufficient to prove that s_2 is inside the model. However, in the ideal case, the surface of a dense point cloud at vertex p_1 is sufficiently smooth and assuming that p_1 is the closest point for a given s_2 between all the points in the model surface, the condition of the negative inner product is sufficient to prove that s_2 is inside the model.

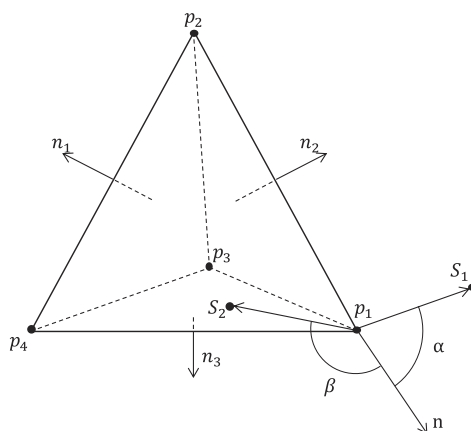


Fig. 4. Illustration of inside–outside classification.

The inside–outside classification algorithm is an effective way to judge whether a point is located inside a point cloud block. The normal vector \vec{n}_p of any point in the model is determined based on the surrounding points and the center of the model. For any sampled point s in the axis-aligned bounding box, we find the closest point p in the point cloud and calculate the inner product between \vec{ps} and \vec{n}_p to judge whether the point s is inside the point cloud block.

With the Monte Carlo method above, when the number of samples N is large enough, the estimated volume of the point cloud block \hat{V}_g is relatively accurate. Specifically, with the assumption that the volume of the goaf is larger than $\frac{1}{3}$ of the bounding box volume, we proved that the confidence level of the hypothesis that the relative error of the volume calculation was lower than 0.1% was over 95% when the number of samples $N > 8,000,000$. The detailed analysis and proofs are presented in the Appendix A.1. This approach is computationally affordable for a high-performance computer to sample and classify each point for such cases. At the same time, sampling and inside–outside classification for each block is completely executed offline before backfilling, and it will not affect the performance for online application.

2.3. Real-time soft-sensing for paste height in backfilling

In Section 2.2, we introduced the method to calculate the volume of each slice in the point cloud based on multiple-cutting operations, Monte Carlo sampling, and the inside–outside classification method. The generated associative table helped to determine the filling height according to the current accumulated volume of paste when the backfilling was under way.

As shown in Fig. 5, we assumed that the height of the goaf was H and the height of each slice was h . The accumulative volume of discharged paste V_{in} was measured by integrating the monitored flow rate f_t from the start time to the current time t . We defined v_i to denote the volume of the i -th slice. The m -th slice in the goaf being backfilled virtually was determined according to the conditions $\sum_{i=1}^{m-1} v_i \leq V_{in}$ and $\sum_{i=1}^m v_i > V_{in}$. The current backfilling height H is estimated as follows:

$$H = \left(m - 1 \right) * h + \frac{V_{in} - (v_1 + v_2 + \dots + v_{m-1})}{v_m} * h. \quad (1)$$

Based on production experience, when the height of the backfilling paste is available, the optimal cement–tailing ratio is also determined. The developed system requires the operator to input the initial cement–tailing ratio R_i , final cement–tailing ratio R_f , and desired backfilling height H_s before backfilling. The recommended cement–tailing ratio R_t is solved by solving a simple linear interpolation:

$$R_t = R_i + \frac{(R_f - R_i)(H - H_i)}{H_s - H_i}, \quad (2)$$

where H_i is the initial paste height before the current backfilling operation. The inferred ratio R_t is transmitted to the intelligent control sys-

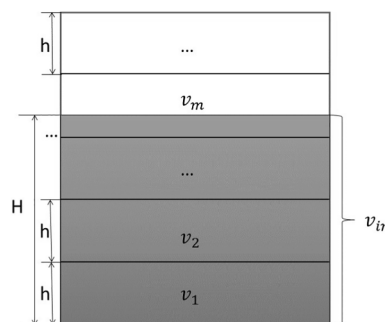


Fig. 5. Filling height calculation of the paste.

tem to regulate the weight of cement based on the current rate of the tailing flow in real time. Despite the employed linear operational strategy being simplified, the precision of the control ratio is acceptable in industrial production. The quality of produced paste is improved, and the cost of cement is reduced significantly.

2.4. Visualization system for paste backfilling

In this paper, we developed an integrated visualization system for backfilling using a Browser/Server architecture. The implementation of the complete system is divided into the backend part and frontend part as shown in Fig. 6.

1) Backend: The backend part is running on a high performance server to provide resources identifications and the analysis of the points cloud model and production data. The FreeOpcUa, an open source OPC software written in Python, is employed to collect the real-time production data from devices in time series format. The data is stored in MongoDB database, which is a NoSQL database with high flexibility and throughput. The system employs Point Cloud Library (PCL) to process 3D point cloud. The utilized functions include format conversion, point downsampling, and inside–outside classification.

As the developed web system follows the Browser/Server architecture, the server side is implemented based on Django framework which is a high-level web development framework in Python and capable of building integrated websites. It handles the web requests and resource identification coming from the frontend.

2) Frontend: The frontend part provides visual information and numerical information of backfilling process in web pages for users. Vue.js, a real-time responsive framework, is employed as the core component in frontend to update the web page dynamically. To display the 3D model of the filled goaf for operators, we introduce the Three.js library to render the 3D model and provide interactive operations on web pages in real-time. By checking the displayed animations and information on the web system, the operators could evaluate the status of real-time productions and make decisions on the backfilling devices.

The system renders the **real-time 3D animations** and **numerical data** of backfilling on the web page. Operators could observe the current status of the production, including **current height, volume, the percentage, and the left duration**. The platform also supports **manifold interactions**, such as dragging and rotation, for providing various perspectives of the filled goaf. Furthermore, the system also analyzes the

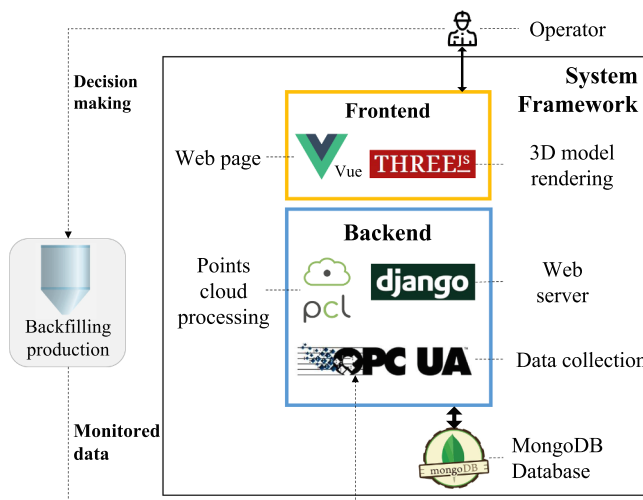


Fig. 6. Implementation of the backfilling visualization system.

accumulative percentage of the backfilling height and infer the **theoretically most saving cement-tailings ratio**, which satisfies the required paste strength. The controlling signal is written into production system automatically based on OPC-UA protocol.

We deployed the complete system and services on a high-performance computer IW4200-4G server with the Ubuntu 16.04 operating system. The computer has 128 GB RAM and two Intel Xeon E5-2620V4 processors.

3. Evaluation in actual backfilling production

To demonstrate the feasibility and accuracy of the proposed soft-sensing algorithm, we examined the backfilling visualization and soft-sensing system with real cemented paste backfilling production on a copper mine setup located at Chambishi in the Copperbelt province of Zambia. Two main research questions are answered in this section: (i) Does the proposed pipeline measure the volume of each slice in goaf model accurately? (ii) Is the soft-measured backfilling height accurate enough for guiding industrial production? First, we introduce the basic information of the experimental goafs and how the 3D point cloud model was scanned by the laser scanner. Next, the detailed experimental results for estimating the volume of the slices and soft-sensing for the backfilling height are discussed. Finally, we will show the screenshots of developed 3D backfilling visualization system, which were captured during backfilling productions.

3.1. Details of goaf and model scanning

The three investigated goafs waiting to be backfilled underwent their last exploitations in August 2019. The person who was responsible for the surveying and mapping activities held a GeoSLAM ZEB-HORIZON 3D laser scanner to collect complete point cloud data of goafs. For each goaf, underground scanning lasted for about 2 h, and each collected point cloud included about 3 million extremely dense points. We aligned the points in the appropriate coordinate system after the evacuation and subsequently removed the outliers and noisy points in the model. Fig. 7 illustrates one of the final goaf models with about 80,000 points from the front and vertical views.

3.2. Slicing and volume calculation

In the first experiment, the goaf shown in Fig. 7 is employed to evaluate the accuracy of the proposed technique for calculating the volumes of the point cloud and slices. The height and the length of the goaf are measured about 11 and 110 m, respectively, corresponding to a volume of about 7652 m³. The comparisons between the multiple cut and single cut were studied. In the single cut experiment, the goaf is merely sliced along height-axis, without further splitting each slice into blocks. In order to estimate the volume of the complete slices in single-cutting experiment, we still employ Monte Carlo sampling, as same as the multiple cut experiment.

Fig. 8 illustrates the accurate volume of the goaf and the estimated volume of twenty slices using the two slicing methods. The comparative results present that the multiple-cut method, which cut the slice into blocks and estimated the volume for each part, outperformed the single-cut method. Most of the error in the single-cut method was from the top and bottom slices because these two regions are irregular and filled with vacancies. In the multiple cut method, after the first slice along the height-axis, we cut each slice along the horizontal axis, and the points in one slice were dispersed into several blocks. As Section 2.2 discussed, whether the cutting plane was located on the vacancy or area filled with points, such as Fig. 3(b), does not affect the proposed method for judging whether the point was in the goaf. This guarantees the accuracy of volume estimation for each slice when we choose the cutting planes uniformly along the long side.

We also conducted an ablation experiment to demonstrate that the

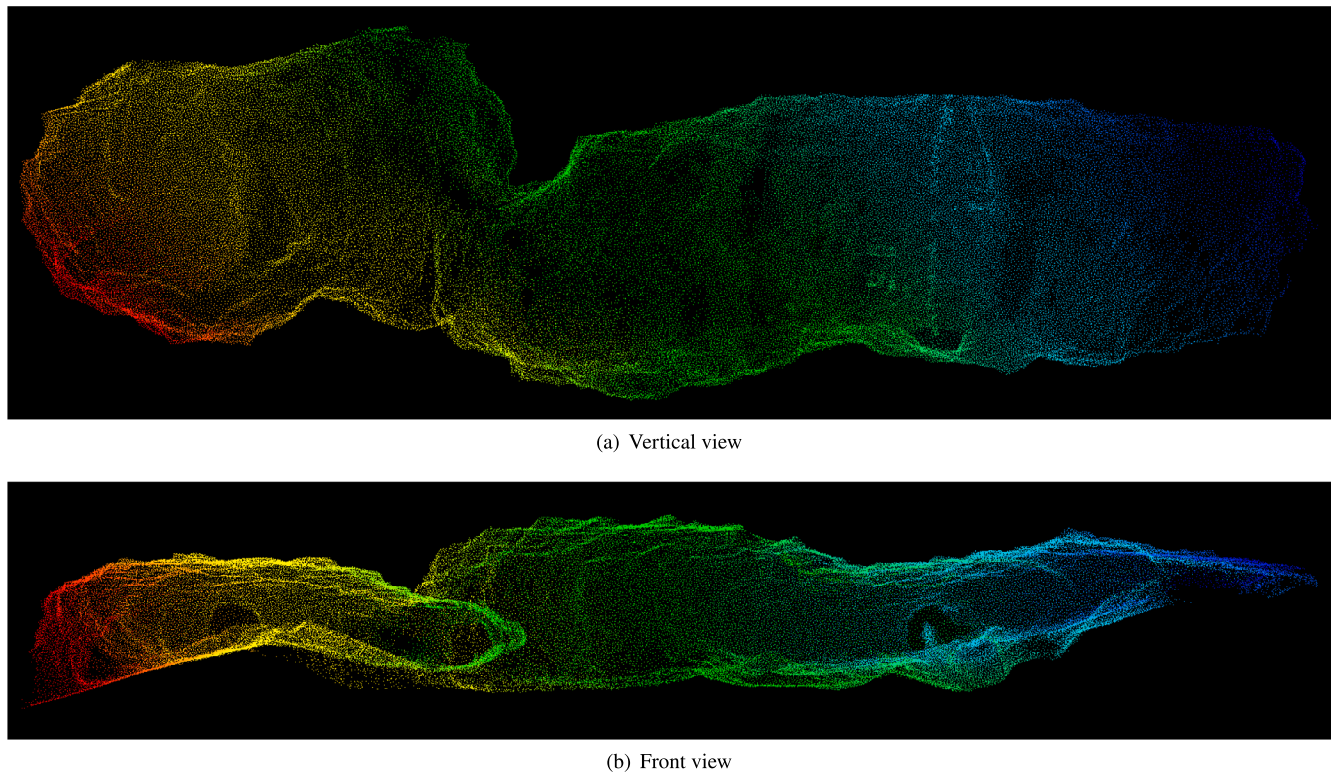


Fig. 7. Point cloud model of goaf obtained by GeoSLAM ZEB-HORIZON.

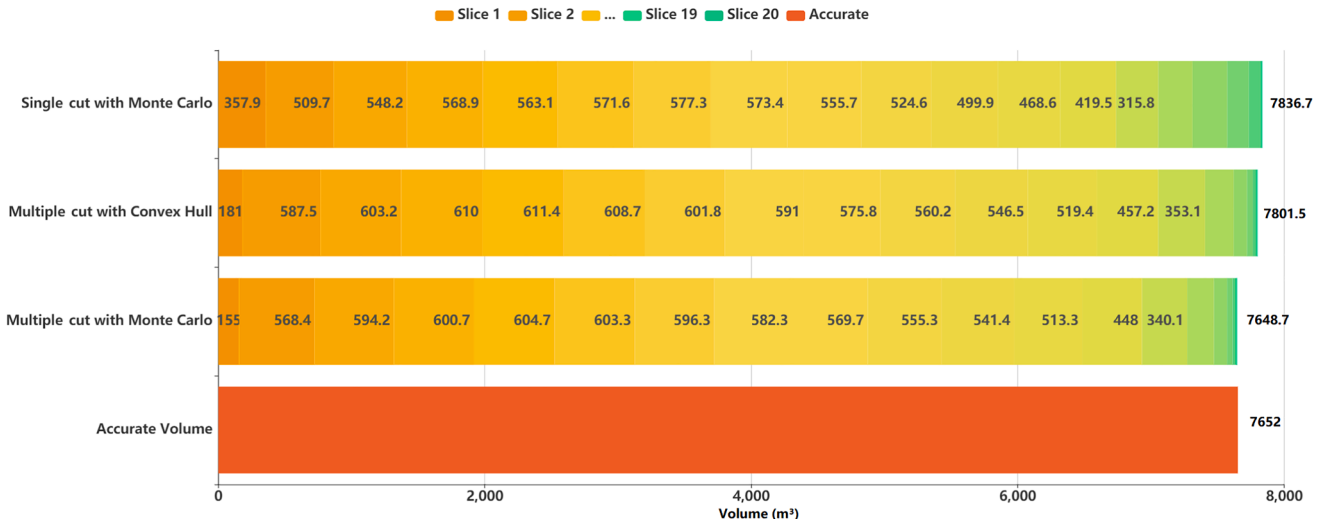


Fig. 8. The comparison of different methods for estimating the volume of goaf and slices.

point-cloud-based Monte Carlo method is a rational choice for estimating the volume of each block. In the ablation study, we reserve the multiple-cutting operation and replace the Monte Carlo method with the convex hull method to measure the volume of each block. The convex hull method builds the convex hull of the points in a block and reconstructs the mesh surface whose volume can be solved directly. The second row in Fig. 8 shows the estimated volume of all the slices based on the convex hull method. The Monte Carlo sampling outperformed the convex hull method significantly. Although the convex hull method does not suffer from statistic deviations like the Monte Carlo method, it finds the smallest convex polyhedron to contain the given point set. However, the real shape of the block could be non-convex, which caused the estimated volume of the block to be slightly larger than the actual

volume, and the magnitude of the error was influenced by the degree of non-convexity. In contrast, the shape of the points in the block did not affect the Monte Carlo calculation and the inside–outside classification method.

3.3. Soft-estimation for Paste height

Next, we will examine the accuracy of the proposed backfilling height estimation algorithm on three actual backfilling goafs. When the backfilling production is ongoing, the real-time flow rate of the pumped paste is monitored with the unit as m^3/h . The proposed soft-sensoring algorithm infers the real-time backfilling height according to the accumulated volume of filled paste and the three-dimensional model of goaf.

In this experiment, we compared the measured and estimated heights for our system on three goafs.

Before backfilling, a retaining wall was built beside the goaf to prevent the leakage of paste. Consecutive backfilling increased the pressure on the retaining wall, which introduced a risk of destroying the wall and causing severe accidents. In general, the complete backfilling procedure for one goaf is scheduled to execute three or four times based on the size of the goaf, which allows time for the paste to harden. Because it is dangerous and difficult to measure the real-time accurate height of paste in the goaf during backfilling, we only collected the ground-truth records when the backfilling system was paused and the filled paste had solidified, which guaranteed that the measurement was relatively accurate and safe.

Fig. 9 and **Table 1–3** illustrate the comparisons of the measured and estimated heights on three goafs. The results demonstrate that the estimated heights are close to the accurate measured height and the accumulated error was less than 10% approximately. Specially, the method still makes accurate estimations, even in the beginning and ending phases, in which the shape of goaf is uniform and the growth rate of paste height is unstable. The estimation error of the proposed method is controlled under 1 m, which is acceptable for guiding the operators to shut down the paste pumping or adjusting the cement–tailings ratio. In the last column in **Table 1–3**, the analyzed optimal cement–tailings ratio according to estimated paste height are presented and written to the cement control system in real-time.

3.4. Cemented paste backfilling visualization system

A cemented-paste backfilling visualization system was developed based on the B/S architecture, which could visualize the original goaf model and provide a detailed animation of the backfilling progress. As shown in **Fig. 10**, the operators are able to monitor all necessary information about backfilling by employing the system, including the following:

1. Complete information about the filled goaf itself, such as the height, volume, and shape of the goaf.
2. The planning of the current backfilling, including the target height and target volume.
3. Measurement of real-time information and some inferred information by soft-sensing, such as the volume, estimated backfilling height, and estimated remaining time.

4. Discussion

Although this study solved the soft-sensing and visualization

Table 1

Tabular evaluation of estimated backfilling height for goaf-1.

Paste volume (m ³)	Accurate height (m)	Estimated height (m)	Absolute error (m)	Relative error	Cement-tailing ratio
2654.56	2.8	3.05	0.25	8.93%	0.11
5122.25	5.1	5.53	0.43	8.43%	0.10
6177.42	6.1	6.68	0.58	9.51%	0.10
7221.86	7.4	8.11	0.71	9.59%	0.10
7647.32	10.5	11.45	0.95	9.05%	0.08

Table 2

Tabular evaluation of estimated backfilling height for goaf-2.

Paste volume (m ³)	Accurate height (m)	Estimated height (m)	Absolute error (m)	Relative error	Cement-tailing ratio
670.78	4.1	4.42	0.32	7.80%	0.12
1759.59	6.7	6.77	0.07	1.04%	0.11
2863.55	8.3	8.76	0.46	5.54%	0.11
4920.42	11.9	12.14	0.24	2.02%	0.10
6804.82	14.2	14.97	0.77	5.42%	0.10
8039.92	15.8	16.78	0.98	6.20%	0.09
9195.91	20.7	21.66	0.96	4.64%	0.08

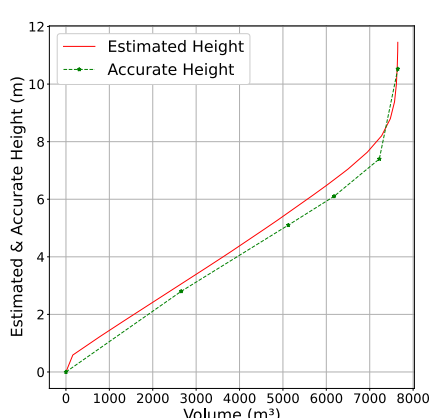
Table 3

Tabular evaluation of estimated backfilling height for goaf-3.

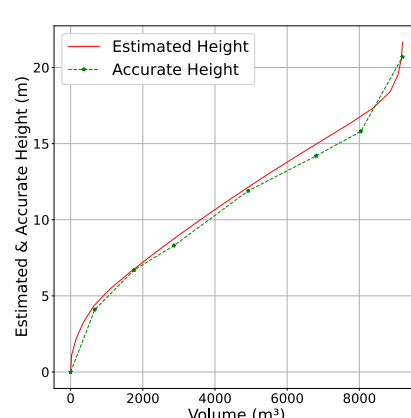
Paste volume (m ³)	Accurate height (m)	Estimated height (m)	Absolute error (m)	Relative error	Cement-tailing ratio
1102.03	2.8	2.99	0.19	6.79%	0.12
2865.79	5.0	5.22	0.22	4.40%	0.12
4948.92	7.1	7.43	0.33	4.65%	0.11
6234.20	8.5	8.67	0.17	2.00%	0.11
8652.72	10.3	10.87	0.57	5.53%	0.10
12256.62	13.3	14.04	0.74	5.56%	0.10
14962.26	15.7	16.58	0.88	5.61%	0.09
17269.60	21.2	22.16	0.96	4.53%	0.08

problem of backfilling preliminarily, three vital issues exist in the real production, which are unavoidable:

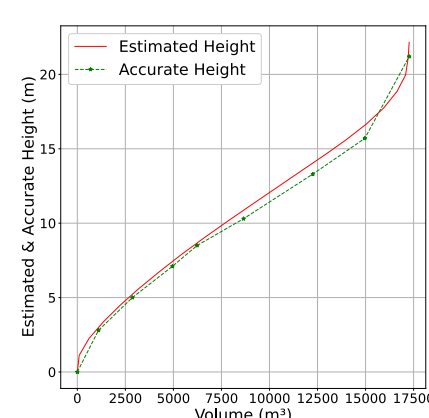
- Filling shrinkage of cemented paste ([Meddah and Tagnit-Hamou, 2009](#)) makes the measured volume of filled paste slightly larger than the accurate volume of filled coagulated paste. The degree of shrinkage is closely related to the internal relative humidity, materials, and ratio of cement to tailings. Correcting the error from paste



(a) goaf-1



(b) goaf-2



(c) goaf-3

Fig. 9. Illustrating the estimated paste height in real-time (red line), the measured points of accurate paste height (green points).

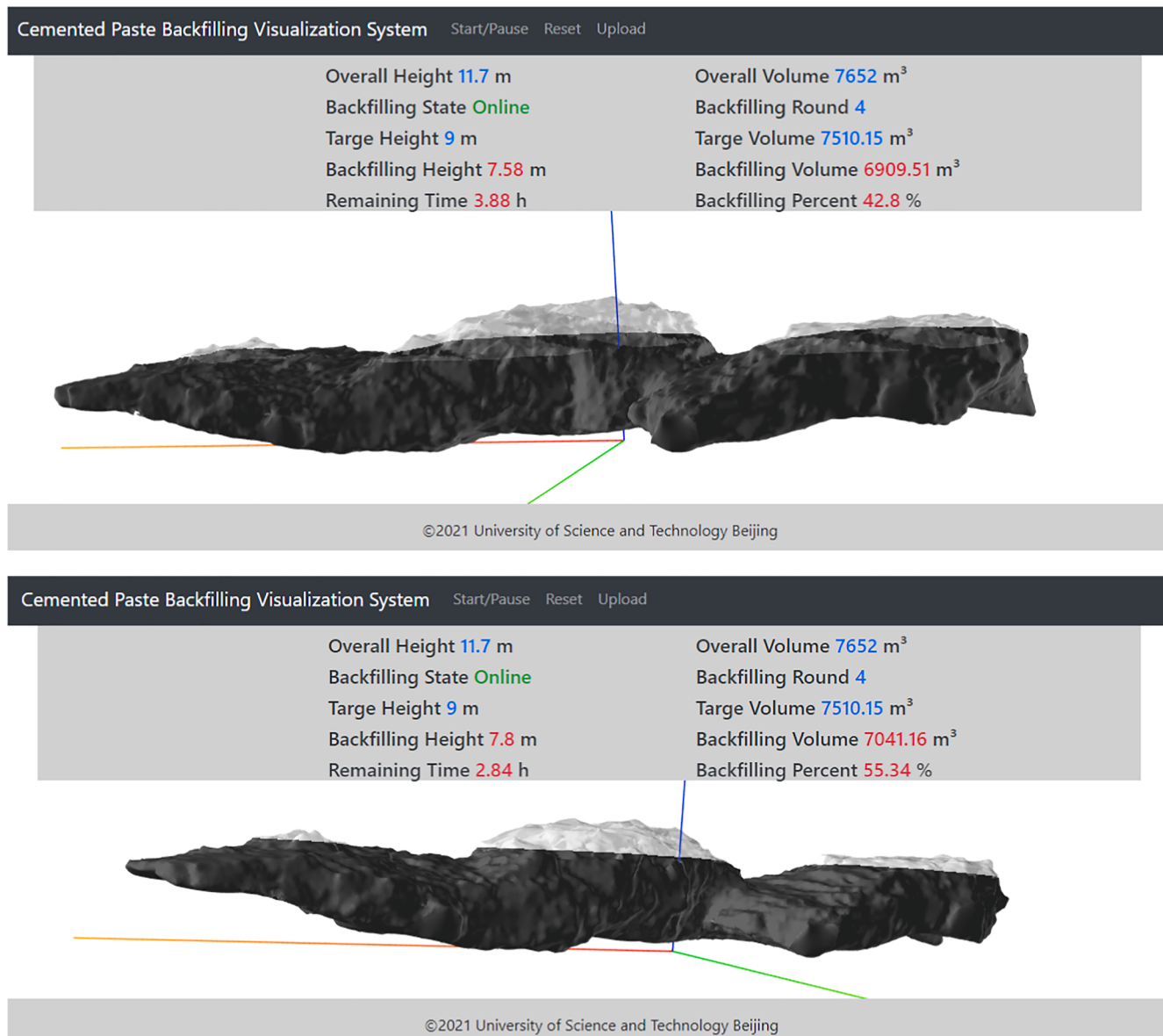


Fig. 10. Backfilling visualization system.

shrinkage using prior technique parameters is a topic for which we have follow-up work planned.

- Paste, as a kind of granular media, has relatively high viscosity and more complex dynamic features compared with water and other Newtonian fluids. The filled paste will form a dynamical cone and spread outward slowly until coagulating. The height of the coagulated paste is related to the distance from the feeding port to each position. Generally, there are several feeding ports distributed on the highest positions in roof that discharge paste together. The proposed pipeline is a reasonable simplification in ideal conditions which assumes that the backfilling heights at all positions are equal. However, this assumption can be further improved by introducing fluid kinematics to simulate the shapes, positions, and velocities of paste particles during backfilling. More vivid visualization results and more accurate instructions for production could be achieved with improvements to the procedure.
- Roof-contacted filling is one of the most critical issues in the backfilling. In most cases, the vent holes are drilled in the highest points of the roof for discharging air, which promotes the roof-contacted backfilling. However, when the vent holes are insufficient or the

positions of the holes are improper, some pressure-tight spaces may be generated, which prevents the goaf to be filled with the produced paste completely. When the roof of the goaf is rugged, unsuccessful roof-contacting appears more frequently and brings potential security risks to the filling body quality. In the actual production, it is difficult to judge whether the filled paste connects the roof. In the future study, the positions of the marked vent holes, the shape of the roof, and the backfilling pressure produced from the height difference between the backfilling pump and the underground goafs are supposed to be incorporated in the analysis of the backfilling progress. The visualization system will provide more detailed roof-contacted information in future version, such as displaying the distributions and the volumes of the pressure-tight spaces.

- The last problem is closely related to production management, which restricts the application of our system in some mining setups. Sometimes, the produced cemented paste is split into several flows to backfill different goafs simultaneously underground. Most monitoring systems cannot capture the accurate volume of the flow in each sub-pipe, which restricts us to estimate the accumulated volume of filled paste in one goaf exactly. Machine learning methods might

be a feasible way to predict the ratio of allocated paste in each pipe according to the historical experience (Yuan and Li, 2022).

5. Conclusion

In this study, a technical pipeline was proposed, and an integrated system for measuring the real-time progress of backfilling was developed. GeoSLAM ZEB-HORIZON, a 3D laser scanner, was utilized to scan the required point cloud data accurately. After preprocessing the original point cloud by filtering, rotating, and a series of operations, we sliced the goaf along the height axis and computed the volume for each slice based on multiple cuts, Monte Carlo sampling, and inside–outside classification. During backfilling, the height of the filled paste could be estimated in real-time by finding the corresponding slice for which the accumulated volume from the bottom was approximately equal to the volume of filled paste. The optimal ratio of cement to tailings was also recommended based on the current backfilling height and manual input parameters. The estimated backfilling height with other progress information is presented in the backfilling visualization platform, which is a web system developed based on the B/S architecture. The proposed technique pipeline and the developed software application solves the problems of shortages of devices and techniques for monitoring the underground backfilling information in real time. More complicated and helpful functions, such as planning for intermittent backfilling, safety assessment warning, and Roof-contact judgement will be committed in future studies.

CRediT authorship contribution statement

Zhaolin Yuan: Writing - Original draft preparation,

Appendix A

A.1. Analysis of deviation and confidence intervals for Monte-Carlo-based volume estimation

According to the definition in Section 2.2, we assume that the volume of the bounding box and point cloud block are V and V_g , respectively. The sampling points are generated repeatedly N times in the bounding box uniformly, and whether the point is in the block or not is a binary random variable that follows a Bernoulli distribution $p(X = 1) = \frac{V_g}{V}$. A binomial distribution $X \sim B(N, \frac{V_g}{V})$ describes the distribution of the number of times the sampled point was located in the block with mean $E(x)$ and variance $D(x)$, defined as follows:

$$\begin{aligned} E(X) &= \frac{NV_g}{V}, \\ D(X) &= \frac{NV_g(V - G_g)}{V^2}. \end{aligned} \tag{3}$$

According to the central limit theorem (CLT) (Wikipedia contributors, 2020), the distribution of X approaches a normal distribution when N is sufficiently large. Thus, the estimated volume of the point cloud model \hat{V}_g follows a normal distribution:

$$\begin{aligned} E(\hat{V}_g) &= \frac{V \times E(X)}{N} = V_g, \\ D(\hat{V}_g) &= \frac{V^2 D(X)}{N^2} = \frac{V^2 \times N \times \frac{V_g}{V} \times \frac{V - V_g}{V}}{N^2} \\ &= \frac{V_g(V - V_g)}{N}. \end{aligned} \tag{4}$$

\hat{V}_g is an unbiased estimate of V_g , and the deviation $D(\hat{V}_g)$ decreases when we increase N , the number of samples, or build a tighter bounding box that minimizes $V - V_g$. To achieve a relative error $\frac{|V_g - \hat{V}|}{V_g}$ that is lower than 0.1% with 95% confidence, we can calculate the minimum N according to the 95% confidence intervals of the standard normal distribution ($-1.96, 1.96$).

$$1.96 * \sqrt{\frac{V - V_g}{NV_g}} \leqslant 0.01 \rightarrow N \geqslant \left(\frac{1.96^2}{0.001} \right) \frac{V - V_g}{V_g}. \tag{5}$$

Conceptualization of this study. **Xiaojuan Ban**: Conceptualization of this study, Methodology. **Fangyuan Han**: Writing, Methodology and Software. **Xingquan Zhang**: Writing and data curation. **Xingquan Zhang**: Methodology and Software. **Shenghua Yin**: Proofreading. **Yiming Wang**: Conceptualization of this study.

Declaration of Competing Interest

The authors declare that they have no known competing financial interests or personal relationships that could have appeared to influence the work reported in this paper.

Acknowledgement

The authors acknowledge financial support from the National Key Research and Development Program of China (No.2019YFC0605300, No.2020YFB0704501), National Natural Science Foundation of China (No.61873299, No.61902022, No.61972028), Fundamental Research Funds for the Central Universities of China (No.FRF-TP-20-061A1Z), the Finance Science and Technology Project of Hainan province (No. ZDYF2020031), Scientific and Technological Innovation Foundation of Shunde Graduate School for USTB (No. BK19AE034), and the Fundamental Research Funds for the University of Science and Technology Beijing (No. FRF-BD-19-012A and No. FRF-TP-19-043A2). The computing work was partly supported by USTB MatCom of Beijing Advanced Innovation Center for Materials Genome Engineering.

Under the reasonable assumption of $V_g \geq \frac{1}{3}V$, we obtain $N \geq 7,683,200$.

References

- Yuan, Zhaolin, Li, Xiaorui, et al., 2022. Continuous-time prediction of industrial paste thickener system with differential ODE-net. *IEEE/CAA Journal of Automatica Sinica* 9 (4), 686–698.
- Adams, B., Dutré, P., 2003. Interactive boolean operations on surfel-bounded solids, in: ACM SIGGRAPH 2003 Papers, pp. 651–656.
- Chen, L.H., Liao, F.Q., Ye, M., 2014. The development and application of 3d monitoring alarm warning system in tunnel construction, in: Applied Mechanics and Materials, Trans Tech Publ. pp. 839–842.
- Cosser, E., Roberts, G.W., Meng, X., Dodson, A.H., 2003. Measuring the dynamic deformation of bridges using a total station. In: Proceeding of the 11th FIG symposium on deformation measurements. Santorini, Greece, pp. 25–28.
- Fuller, A., Fan, Z., Day, C., Barlow, C., 2020. Digital twin: Enabling technologies, challenges and open research. *IEEE Access* 8, 108952–108971.
- Hu, D.T., Cen, Y.G., Yang, Z., Huang, L., 2013. The development and application of digital mine ventilation system, in: Applied Mechanics and Materials, Trans Tech Publ. pp. 1844–1850.
- Li, H., Wu, A., Wang, H., 2019. Evaluation of short-term strength development of cemented backfill with varying sulphide contents and the use of additives. *J. Environ. Manage.* 239, 279–286.
- Liu, M., Fang, S., Dong, H., Xu, C., 2021. Review of digital twin about concepts, technologies, and industrial applications. *Journal of Manufacturing Systems* 58, 346–361.
- Lu, H., Qi, C., Chen, Q., Gan, D., Xue, Z., Hu, Y., 2018. A new procedure for recycling waste tailings as cemented paste backfill to underground stopes and open pits. *Journal of Cleaner Production* 188, 601–612.
- Lu, H., Zhang, S., 2017. Design of roof-contacted filling ratio and filling holes in the sublevel open stoping with subsequent filling method. *International Journal of Mining and Mineral Engineering* 8, 265–279.
- quan LUO, Z., jie HUANG, J., yan LUO, Z., WANG, W., guang QIN, Y., 2016. Integration system research and development for three-dimensional laser scanning information visualization in goaf. *Transactions of Nonferrous Metals Society of China* (English Edition) 26, 1985–1994.
- Meddah, M.S., Taghit-Hamou, A., 2009. Pore structure of concrete with mineral admixtures and its effect on self-desiccation shrinkage. *ACI Mater. J.* 106, 241–250.
- Mishra, P., Pratik, Kumar, M., Kumar, S., Mandal, P., 2018. Wireless real-time sensing platform using vibrating wire-based geotechnical sensor for underground coal mines. *Sensors and Actuators A: Physical* 269, 212–217.
- Núñez, F., Langarica, S., Díaz, P., Torres, M., Salas, J.C., 2020. Neural Network-Based Model Predictive Control of a Paste Thickener over an Industrial Internet Platform. *IEEE Trans. Industr. Inf.* 16, 2859–2867.
- Qi, C., Chen, Q., Fourie, A., Zhao, J., Zhang, Q., 2018. Pressure drop in pipe flow of cemented paste backfill: Experimental and modeling study. *Powder Technol.* 333, 9–18.
- Qi, C., Fourie, A., Chen, Q., Zhang, Q., 2018. A strength prediction model using artificial intelligence for recycling waste tailings as cemented paste backfill. *Journal of Cleaner Production* 183, 566–578.
- Tao, F., Zhang, H., Liu, A., Nee, A.Y., 2018. Digital twin in industry: State-of-the-art. *IEEE Trans. Industr. Inf.* 15, 2405–2415.
- Vachalek, J., Bartalsky, L., Rovny, O., Sismisova, D., Morhac, M., Loksik, M., 2017. The digital twin of an industrial production line within the industry 4.0 concept. *Proceedings of the 2017 21st International Conference on Process Control, PC 2017*, 258–262.
- Wang, Y., Zheng, G., Wang, X., 2019. Development and application of a goaf-safety monitoring system using multi-sensor information fusion. *Tunn. Undergr. Space Technol.* 94, 103112.
- Wikipedia contributors, 2020. Central limit theorem — Wikipedia, the free encyclopedia. https://en.wikipedia.org/w/index.php?title=Central_limit_theorem&oldid=996445291. [Online; accessed 18-January-2021].
- Wu, A., Ruan, Z., Bürger, R., Yin, S., Wang, J., Wang, Y., 2020. Optimization of flocculation and settling parameters of tailings slurry by response surface methodology. *Miner. Eng.* 156, 106488.
- Yin, S., Shao, Y., Wu, A., Wang, H., Liu, X., Wang, Y., 2020. A systematic review of paste technology in metal mines for cleaner production in China. *Journal of Cleaner Production* 247, 119590.
- Yuan, Z., Hu, J., Wu, D., Ban, X., 2020. A dual-attention recurrent neural network method for deep cone thickener underflow concentration prediction. *Sensors* 20, 1260.
- Zhou, Y.D., Li, Z.X., Li, C.P., Cao, Z.G., 2012. Design and realization of mine water-inrush visualization simulation system. In: Advanced Materials Research, Trans Tech Publ. pp. 6632–6640.